

# Three-Dimensional Core-Shell Superstructures: Mechanically Strong Aerogels

NICHOLAS LEVENTIS

Department of Chemistry, University of Missouri, Rolla, Missouri 65409

Received October 26, 2006

## ABSTRACT

Nanocasting conformal polymer coatings on preformed three-dimensional assemblies of nanoparticles, macroscopically classified as aerogels, reinforces the interparticle necks and increases the strength of the bulk material dramatically. For example, specific compressive strengths are reported to be higher than those for mild steel and aluminum, while the ability to store energy may surpass that of armor grade ceramics. Specific chemistries have been developed for cross-linking skeletal nanoparticles with polyureas and polyurethanes, epoxies, and polystyrene, while the technology has been demonstrated with 30 different nanoparticle networks in addition to silica.

## 1. Introduction

From a materials perspective, nanotechnology uses molecular science (chemistry and physics) to manipulate matter in the 1–100 nm size regime in order to furnish useful macroscopic properties. In that regard, improvements in performance in terms of strength, modulus, and wettability are accomplished by, for example, introducing nanoparticles as fillers in plastics.<sup>1</sup> Materials compatibility is improved by chemical bonding of the filler with the polymer, enhancing properties beyond what is obtained by simple mixing.<sup>2,3</sup> Going a step further, that is if both the dopant and the matrix consist of particles with similar sizes, we may realize distinct advantages in certain applications, for example, in catalysis.<sup>4</sup> On the basis of this background, if the dopant and the matrix (i.e., the filler and the polymer) are not only sized similarly, but also if the relative amounts are comparable, their roles can be reversed. Then, if the filler, or one of its forms, possesses interesting properties of its own, those properties could be enhanced by chemical nanocasting of a conformal

Nicholas Leventis was born in Athens, Greece, in 1957. He received his B.S. degree in chemistry from the University of Athens in 1980 and his Ph.D. in organic chemistry/photochemistry from Michigan State University (East Lansing, MI) with Peter Wagner in 1985. He spent three years as postdoctoral fellow with Mark Wrighton at the Massachusetts Institute of Technology (Cambridge, MA), and he worked for six years in the private sector before coming to the Chemistry Department of the University of Missouri—Rolla (UMR) as an Assistant Professor in 1994, advancing to Associate Professor in 1999 and to Professor in 2007. Dr. Leventis was introduced to aerogels by Debra Rolison at NRL where he spent the summer of 1998 as a Senior Faculty Fellow. During an extended leave from UMR (September 2002 to February 2006), Dr. Leventis joined as a Civil Servant (GS-14 promoted to GS-15 in June 2005) the Polymers Branch of the NASA Glenn Research Center (Cleveland, OH), where he directed research on polymer-cross-linked aerogels. Dr. Leventis has been the recipient of the ACS Arthur K. Doolittle Award (1992), the NASA Exceptional Scientific Achievement Medal (2005), and one of the 2005 Nano50 Awards. Besides aerogels, his interests include physical organic chemistry, electrochemistry, polymers, and inorganic materials.

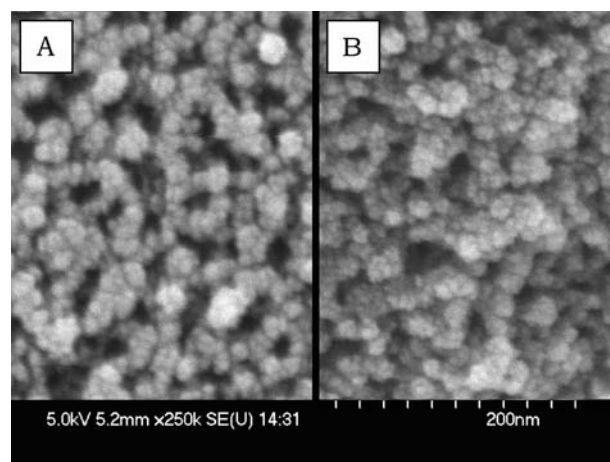
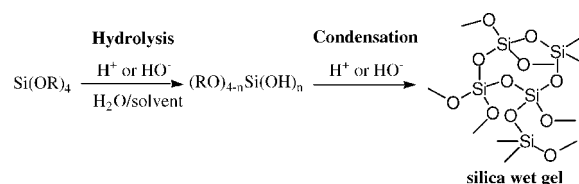


**FIGURE 1.** Scanning Electron Micrographs (SEM) at random spots in the interior of fractured monoliths of: (A) a native base-catalyzed silica aerogel with bulk density  $\rho_b = 0.169 \text{ g/cm}^3$ ; and, (B) a similar sample whose skeletal framework has been coated conformally with a diisocyanate-derived polymer by a process referred to herewith as cross-linking,  $\rho_b = 0.380 \text{ g/cm}^3$ . Reprinted in part with permission from ref 16. Copyright 2002 American Chemical Society.

polymer coating around the filler, fusing the filler particles together. For reasons that become evident below, we refer to this process as cross-linking, and as such a “filler,” we identified silica in its lowest bulk-density form, the silica aerogel.

Silica aerogels are mesoporous materials<sup>5</sup> made by supercritical fluid (SCF) drying of wet gels.<sup>6–9</sup> The latter are prepared via the so-called sol-gel process,<sup>6–8</sup> which usually involves acid- or base-catalyzed hydrolysis and condensation of silicon alkoxides:



where R is  $\text{CH}_3$  for TMOS and R is  $\text{CH}_3\text{CH}_2$  for TEOS.

Just before drying, gelation solvents filling the mesopores are exchanged with liquid  $\text{CO}_2$  in an autoclave, whose temperature is then raised above the critical point of  $\text{CO}_2$  (32 °C, 73.8 bar), turning the entire volume of the liquid into a SCF, which is vented off isothermally (e.g., at 40 °C). That process circumvents evaporation and prevents formation of a liquid–gas interfacial meniscus retreating through the pores of the wet gel. Hence, since no surface tension forces are ever exerted on the skeletal framework, as for example via evaporation during ambient-pressure drying, SCF drying leaves the geometric dimensions of the wet gel unchanged, and the resulting materials are very low density objects (0.003–0.8  $\text{g/cm}^3$ ).

Microscopically, typical base-catalyzed silica aerogels consist of randomly distributed pearl-necklace-like strings

\* Telephone: (573) 341-4391. E-mail: leventis@umr.edu.

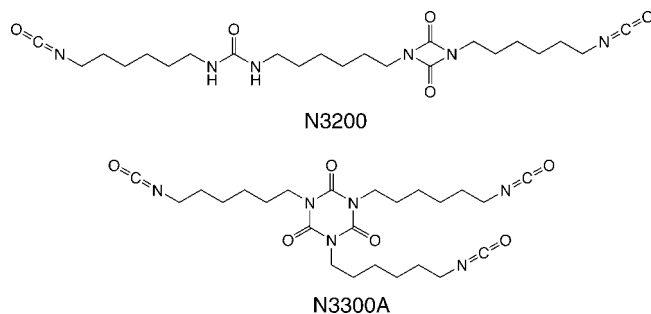
of nanoparticles (Figure 1A).<sup>6–8</sup> Because of that microstructure, silica aerogels can be considered as quasi-stable three-dimensional assemblies of nanoparticles pursued because of useful properties above and beyond those of their individual building blocks. Those properties are traced to the internal voids (dark areas in Figure 1A) and include a very low thermal conductivity ( $<0.020 \text{ W m}^{-1} \text{ K}^{-1}$ ),<sup>8</sup> a low dielectric constant (as low as 1.5),<sup>10</sup> and a high impedance to acoustic waves (with speeds of sound as low as 100 m/s).<sup>11</sup>

Despite those attractive properties, however, aerogels have found only limited use in some very specialized environments, for example, as Čerenkov radiation detectors in certain nuclear reactors, as collectors of hypervelocity particles in space (NASA's Stardust program), and as thermal insulators of the electronic boxes aboard all three NASA Mars rovers (Sojourner in 1997, Spirit in 2004, and Opportunity also in 2004). Wider commercial use of aerogels has been difficult because of their fragility, environmental instability (hydrophilicity), and the need for SCF drying.<sup>8</sup> We could conceivably survive with the first two issues, but the fragility problem imposes severe limitations in terms of handling and long-term use.

This account summarizes our efforts to improve the mechanical properties of aerogels with minimal penalty in the internal void space.

## 2. Mechanically Strong Silica Aerogels by Cross-Linking with Isocyanate-Derived Polymers

Formally, aerogels are low-density foams, and as such, they comprise a subcategory of cellular solids, the strength of which is related to their pore size,<sup>12</sup> increasing with the wall thickness and decreasing with pore diameter. However, the pore walls of base-catalyzed silica aerogels have well-defined weak points, the interparticle necks (Figure 1A). Therefore, although grafting material on the surface of the skeletal nanoparticles will increase stiffness (resistance to bending), to impart a significant increase in strength the grafting material should also bridge the particles at the necks with covalent bonds. This line of reasoning is akin to processes taking place during aging of wet gels, where Ostwald ripening with dissolution and reprecipitation of silica at surfaces with negative curvature (i.e., at surfaces that cross all tangent planes at every point of those surfaces, e.g., the necks) result in mechanically stronger frameworks.<sup>13,14</sup> In our first attempt to address the aerogel fragility issue, this logic was applied by bridging nanoparticles using polyurethane chemistry where the hydroxyl-rich surface of a preformed (from TMOS) silica framework plays the role of a polyol that reacts with a di- and a triisocyanate (e.g., Desmodur N3200 and N3300A, respectively, from Bayer) dissolved in the pore-filling solvent, forming carbamate (urethane).<sup>15–17</sup> As it turns out, the cross-linking reaction requires heating at whatever temperature is allowed by the solvent (e.g., 50 °C with acetone, 70 °C with CH<sub>3</sub>CN, and 100 °C with propylene carbonate); results, however, do not seem to depend on the cross-linking solvent or the specific temperature. At the end, after SCF drying and despite a bulk density increase by a factor of 2.2, the smallest



features in the SEM of a native sample (Figure 1A) are still visible in the SEM of the corresponding cross-linked sample (Figure 1B), leading to the conclusion that the new material covers the skeletal nanoparticles conformally.<sup>15–17</sup> Nitrogen sorption porosimetry yields typical type IV isotherms for both native and cross-linked samples, ensuring that the material remains mesoporous. As demonstrated in Figure 2, this

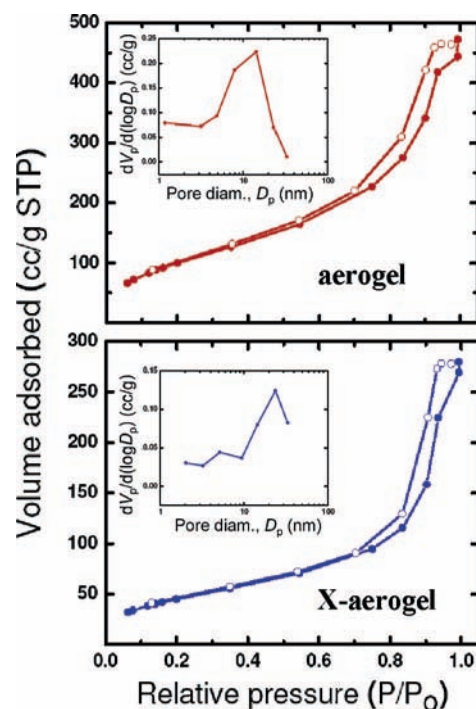


**FIGURE 2.** N<sub>2</sub> sorption isotherms and the corresponding BJH (desorption) pore size distribution data for typical native and cross-linked aerogel monoliths: (●) adsorption and (○) desorption. The specific data are for Gd aerogels (see Section 3.b), where before cross-linking,  $\rho_b = 0.18 \text{ g/cm}^3$  and  $\sigma = 383 \text{ m}^2/\text{g}$ , while after crosslinking,  $\rho_b = 0.44 \text{ g/cm}^3$  and  $\sigma = 171 \text{ m}^2/\text{g}$ .

behavior is typical for all types of aerogels investigated in these studies. The pore size distribution of silica aerogels determined by the BJH method shows a shift toward larger average pore diameters (from 13.4 nm for native aerogels with a bulk density  $\rho_b$  of 0.17 g/cm<sup>3</sup> to 21.9 nm for cross-linked samples with a  $\rho_b$  of 0.39 g/cm<sup>3</sup>), suggesting that access to the smaller crevices on the superstructure has been blocked.<sup>15–17</sup> Consistent with this model is also the decrease in the BET surface area ( $969 \pm 30 \text{ m}^2/\text{g}$  before to  $277 \pm 30 \text{ m}^2/\text{g}$  after cross-linking at a  $\rho_b$  of 0.399 g/cm<sup>3</sup>) with a simultaneous decrease in the C parameter (from 80–90 to 46–48), indicating a decrease in surface polarity, as expected

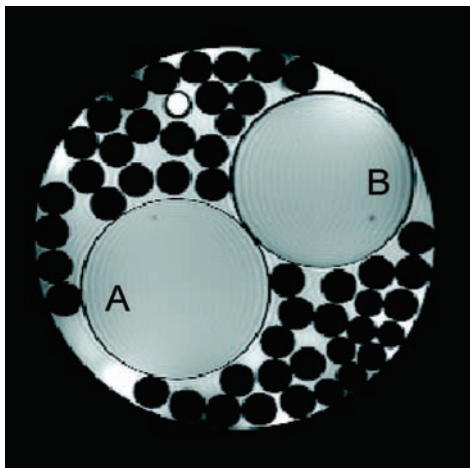


**FIGURE 3.** Cross-sectional MRI of (A) a cylindrical native silica wet gel monolith [diameter of  $\sim 1$  cm, bulk density of the resulting aerogel ( $\rho_b$ ) of  $\sim 0.18$  g/cm $^3$ ] and (B) a similar isocyanate polymer-cross-linked wet gel monolith (diameter of  $\sim 1$  cm,  $\rho_b$  of  $\sim 0.55$  g/cm $^3$ ), both solvent-exchanged and filled with acetone. Smaller dark circles (at two different sizes) surrounding the wet gels are empty capillary tubes helping the monoliths stand straight up. The bright circle at the top is a capillary tube filled with water. The average dark pixel density around the perimeter of the native gel is  $160 \pm 8$  and that of the cross-linked gel  $152 \pm 8$ . The background is  $193 \pm 10$ . Reprinted from ref 17, Copyright 2004, with permission from Elsevier.

for the coating of silica with an organic polymer.<sup>18</sup> It should be pointed out though that in spite of the apparent substantial changes taking place at the nanoscopic level, the accessible (i.e., useable) porosity from a macroscopic viewpoint has not been compromised significantly: NMR imaging (MRI, Figure 3) followed by gray scale analysis shows that the void space available to a solvent (acetone) has been reduced by only  $\sim 5\%$ .<sup>17</sup>

The amount of material incorporated into silica can be controlled to a certain extent by the concentration of the isocyanate in the cross-linking bath, and although the density of a typical cross-linked aerogel monolith may increase by a factor of 3, the strength at breakpoint through a short beam three-point bent test method increases by a factor of up to 300.<sup>19</sup> Typical load-deformation curves and cumulative strength data are summarized in Figure 4. Thus, a typical native sample fails with less than 100 g of vertical force, while a cross-linked sample can withstand in excess of 30 kg (Figure 4A). In fact, cross-linked wet gels can withstand capillary forces, and they can be dried from low-surface tension solvents (e.g., pentane) under ambient pressure, practically without loss of porosity or surface area.<sup>19</sup> Now, as the density (i.e., the amount of material accumulated) increases, cross-linked monoliths become not only stronger (they can withstand more load before reaching the breakpoint) but also stiffer (the initial slope of the load-deformation curve increases) and tougher (they can store more energy as the area under the load-deformation curve also increases). Figure 4B shows that strength increases faster by addition of cross-linker onto the preformed skeletal framework than by use of more TMOS in the sol. In other words, in terms of strength, it is better to achieve a given

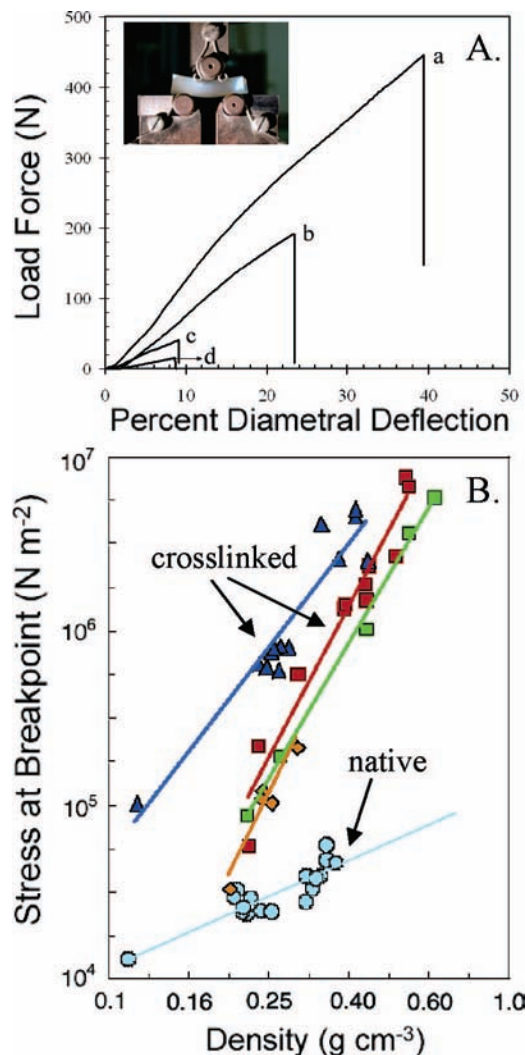


**FIGURE 4.** Mechanical properties (by a short beam three-point bending, see the inset) of isocyanate-cross-linked aerogels and their non-cross-linked (native) counterparts: (A) (a) 0.63, (b) 0.44, (c) 0.38, and (d) 0.28 g/cm $^3$ . Native samples are not shown because they do not register on the load force scale shown. (B) Cumulative data. Blue triangles and the dark blue line concern two-step aerogels (see the text). All other samples use one-step base-catalyzed silica. Multiple lines for cross-linked samples correspond to different di- and triisocyanate cross-linkers. Reprinted from ref 17, Copyright 2004, with permission from Elsevier.

density with a silica-polymer combination rather than with silica alone.

Chemically, the situation turned out somewhat more complex than originally planned. CP-MAS  $^{13}\text{C}$  NMR (Figure 5) shows that the accumulated material contains both carbamate and urea, and Scheme 1 summarizes the mechanistic interpretation: cross-linking involves not only formation of carbamates with surface silanols but also formation of urea by hydrolysis of dangling isocyanates into amines, which in turn react with more isocyanate in the mesopores.<sup>17</sup> On the basis of density increase considerations, the average polymeric tether (from N3200) is  $\sim 5$  monomer units long. The hydrolysis of dangling isocyanates is carried out by gelation water remaining adsorbed on silica even after numerous solvent exchange steps. No unbound polymer is formed in the cross-linking

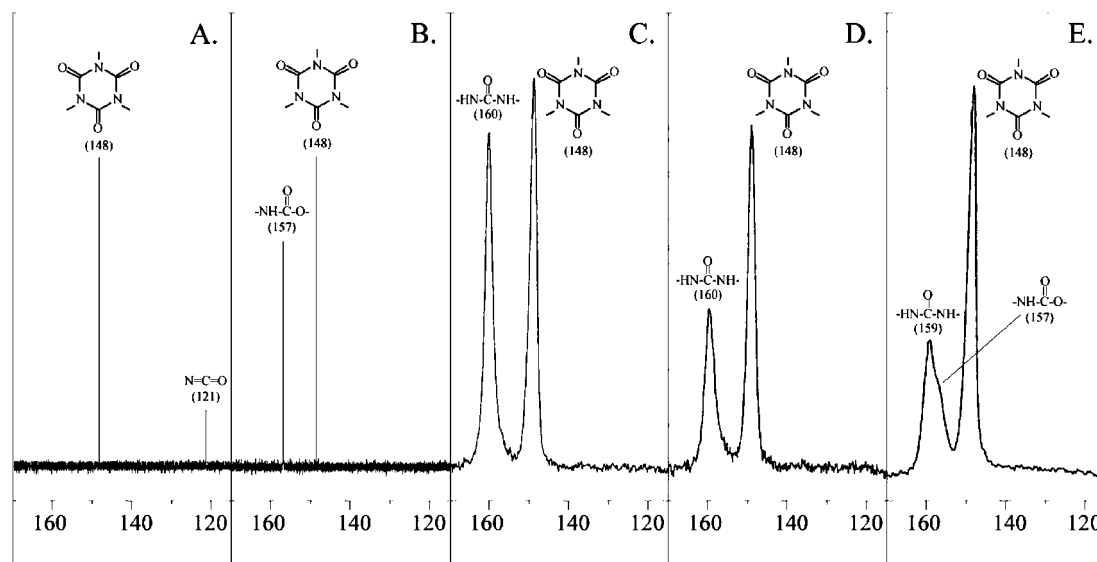
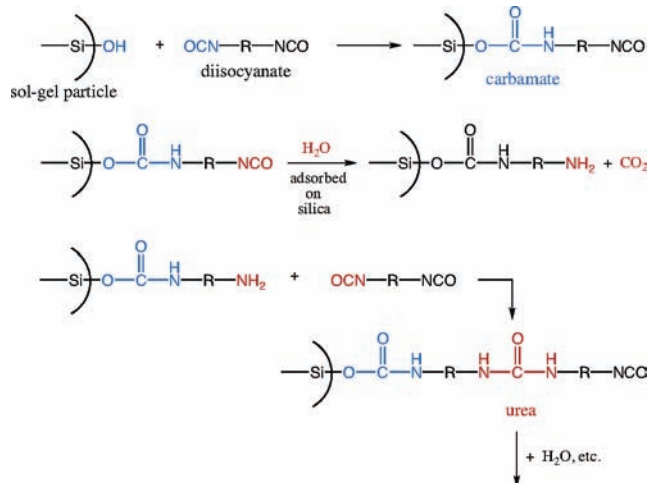


**FIGURE 5.** CP-MAS  $^{13}\text{C}$  NMR characterization of the carbonyl region of (A) N3300A ( $\text{CDCl}_3$ ), (B) the product of the reaction of N3300A with methanol ( $\text{CDCl}_3$ ), (C) the product of the reaction of N3300A with isopropylamine (solid sample), (D) the product of the reaction of N3300A and water (solid sample), and (E) the N3300A cross-linked aerogel with a  $\rho_b$  of  $\sim 0.38 \text{ g/cm}^3$  (solid sample). Reprinted from ref 17, Copyright 2004, with permission from Elsevier.

### Scheme 1. Mechanism of Cross-Linking a Silica with a Diisocyanate<sup>a</sup>



<sup>a</sup> Reprinted from ref 17, Copyright 2004, with permission from Elsevier.

bath under the same conditions. All containers develop pressure during the cross-linking reaction, and the identity of the evolving gas ( $\text{CO}_2$ ) was confirmed by FTIR. In certain experiments involving two-step gels (acid-catalyzed hydrolysis followed by base-catalyzed gelation<sup>20</sup>), reducing the amount of gelation water hampered the ability of wet gels to cross-link.<sup>17</sup> On the other hand, cutting down the number of postgelation wash steps had the opposite effect, yielding denser gels with a progressive loss of porosity.<sup>21</sup> Of course, our data do not exclude the possibility that a certain amount of polymer is surface-bound by one end only. Cross-linked aerogels, however, do not contain free isocyanate (by  $^{13}\text{C}$  NMR and IR), suggesting that all dangling tethers are eventually hydrolyzed and terminated with amine.

The cross-linked aerogels described above are distinctly different from reinforced sol-gel materials by interpenetrating organic polymers with no provisions for covalent

bonding between the two components.<sup>22</sup> By the same token, however, it is also noted that the benefit from developing even weak hydrogen bonding between an interpenetrating polymer (e.g., poly-2-vinylpyridine) and surface silanols has not gone unnoticed.<sup>23</sup> On the other hand, polymer cross-linking as defined here is conceptually related to Einarsrud's work on reinforcing aerogels by rendering interparticle necks wider via postgelation treatment of silica with TEOS.<sup>24</sup> Nevertheless, although silica itself has a high compressive strength, reinforcing silica with silica does not realize the synergistic benefit of reinforcing necks with a high tensile strength material like a polymer. In this context, rubbery materials produced by reactive incorporation of hydroxyl-terminated polydimethylsiloxane (PDMS) in both xerogels and aerogels have been discussed by Mackenzie in terms of three models; at one extreme, silica particles separated from one another are yet connected by PDMS, while at the other extreme, silica particles are in contact with each other and also bridged (cross-linked in our terminology) with PDMS.<sup>25,26</sup> The shortcoming of using a sol incorporating a cross-linker that competes for the same functional groups (Si-OH) involved in gelation is that it provides no control for tuning-in high stiffness and strength versus rubbery behavior. This kind of issue was encountered when the isocyanate was included in our sol: gelation was retarded tremendously (days instead of minutes), while the mechanical properties of the resulting aerogels did not improve significantly.<sup>16</sup>

### 3. Three Degrees of Freedom in the Design of Cross-Linked Aerogels

Once it was evident that interparticle tethers consist of polyurea, the immediate question became whether urea formation can be induced from the attachment point on

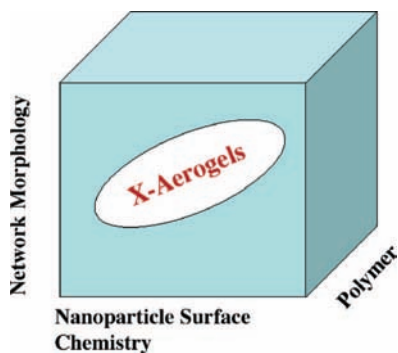


**FIGURE 6.** Design space of crosslinked X-aerogels.

the skeletal framework. Of course, that requires amine-rich mesoporous surfaces, but once we found ourselves willing to consider modification of the surface functionality, we also realized that actually there are three degrees of freedom in the design of cross-linked aerogels (Figure 6): (a) the nanoparticle surface chemistry, (b) the chemical identity of the cross-linker, and (c) the network morphology. Surface and cross-linking chemistries are intimately related and are reviewed together in section 3.a, while section 3.b discusses the effect of the network morphology.

**3.a. Cross-Linking of Amine-Modified Silica.** Amines were introduced into silica by cogelation of TMOS with aminopropyltriethoxysilane (APTES) in a 3:1 volume ratio



(4.8:1 molar ratio). The amount of gelation water was left at approximately the same ratio that was used for the one-step base-catalyzed TMOS gels of the previous section, namely at a 2.2:1  $\text{H}_2\text{O}:(\text{TMOS}+\text{APTES})$  molar ratio. The preferred gelation solvent was acetonitrile. We will refer to this sol formulation as “standard”. The resulting amine-modified silica wet gels were cross-linked with isocyanates,<sup>21,27–29</sup> epoxies,<sup>30</sup> and styrene<sup>31</sup> as outlined in Figure 7. Cross-linked wet gels were dried with SCF  $\text{CO}_2$ .

APTES amines catalyze the sol–gel process, and our TMOS/APTES system gels almost instantaneously upon mixing. To allow time for pouring into molds, sol precursors are cooled in an ice/water or dry ice/acetone (preferred) mixture. Gelation into clear gels takes place in less than a minute while the sol is still cold. It is known that under basic conditions hydrolysis of  $\text{R-Si}(\text{OCH}_3)_3$ , where R is a nonbase group, is slower than hydrolysis of TMOS, resulting in a stepwise sol–gel process, whereas R is grafted onto TMOS-derived silica particles.<sup>7</sup> However, because of the fast reaction (reported as precipitation) of TMOS in the presence of APTES, the TEOS/APTES system has been studied more thoroughly, and it has been reported that hydrolysis of TEOS and APTES take place at similar rates, resulting in gels in which APTES is incorporated into the silica network.<sup>32</sup> In our CP-MAS  $^{29}\text{Si}$  NMR studies (Figure 8), silicas derived from the TMOS/APTES system show clearly that silicon from TMOS is divided between  $\text{Q}^4$ ,  $\text{Q}^3$ , and  $\text{Q}^2$  sites (participating in four, three, and two Si–O–Si bridges, respectively), while practically all the APTES/silicon form is bound through three Si–O–Si bridges ( $\text{T}^3$  silicon at  $-65.1$  ppm) and could be either buried in the

interior or located at the particle surface.<sup>29</sup> The fact, however, that gelation of the TMOS/APTES system is extremely fast while APTES itself apparently hydrolyzes on a time scale of TEOS (10–50 min) suggests that APTES in our TMOS/APTES system is simply grafted on the surface of TMOS-derived particles. The BET specific surface areas,  $\sigma$ , of standard TMOS/APTES aerogels (top of Figure 9,  $\rho_b = 0.190 \pm 0.014$   $\text{g}/\text{cm}^3$ ) are  $\sim 740$   $\text{m}^2/\text{g}$ , larger than values reported for TEOS/APTES gels ( $< 300$   $\text{m}^2/\text{g}$ ).<sup>32</sup> On the basis of skeletal densities of TMOS/APTES aerogels ( $\rho_s = 1.74$   $\text{g}/\text{cm}^3$ ), the particle radius ( $r = 3/(\rho_s\sigma)$ ) is calculated to be 2.3 nm, which is significantly smaller than what has been reported based on SAXS for the TEOS/APTES system (6.0–6.3 nm). The reaction-limited monomer–cluster growth mechanism for gelation in basic media prescribes fast condensation and large particles.<sup>7</sup> The small particles observed herewith are attributed to hydrogen bonding stabilization of the relatively more acidic TMOS-derived Q-hydroxyls by APTES amines.<sup>32</sup>

**3.a.1. Cross-Linking with Isocyanates.**<sup>27–29</sup> Wet gels made using the standard TMOS/APTES formulation followed by (a) four  $\text{CH}_3\text{CN}$  washes to remove excess gelation water, (b) equilibration in a concentrated isocyanate bath (24 h) and oven heating in fresh  $\text{CH}_3\text{CN}$  for 3 days at 71  $^\circ\text{C}$ , and (c) SCF  $\text{CO}_2$  drying resulted in translucent (as opposed to opaque) aerogels with densities in the range of  $0.48 \pm 0.01$   $\text{g}/\text{cm}^3$  (Figure 9, middle), thermal conductivities ( $\sim 0.041 \pm 0.001$   $\text{W m}^{-1} \text{K}^{-1}$ ) comparable to that of glass wool, and an average specific compressive strength at ultimate failure (77% strain, Poisson ratio = 0.18) at  $3.89 \times 10^5$   $\text{N m kg}^{-1}$ , that is 2.8 and 3.2 times higher than that of 4031 steel and of 2024 T3 aluminum, respectively.<sup>33</sup> Clearly, the combination of mechanical and thermal properties of those materials is promising for practical applications. More recent studies have focused on two objectives: (a) exploring properties of low-density cross-linked aerogels ( $\rho_b < 0.1$   $\text{g}/\text{cm}^3$ ) and (b) studying the effect of the preparation protocol on the properties of the final product. To minimize the number of samples required for those studies, we made extensive use of statistical design-of-experiments (DoE) methods, whereas a subset of experimental runs fully capable of capturing with a high degree of confidence the relationships between properties and preparation conditions is computer-generated from all possible candidate experiments.<sup>30</sup> Here we summarize results that shed light on the chemical composition of the materials.

Low-density APTES-modified aerogels were prepared by reducing the concentration of total silica (TMOS and APTES) while keeping the TMOS:APTES volume ratio at 3:1. Since APTES-modified silica reacts with isocyanate even at ambient temperature, cross-linking was carried out and investigated at two temperature extremes: 71 and 25  $^\circ\text{C}$ .<sup>28</sup> Low-density cross-linked aerogels ( $\sim 0.05$   $\text{g}/\text{cm}^3$ ), irrespective of preparation conditions, are flexible, and microscopically, they include more empty space than denser versions (bottom vs middle of Figure 9) with porosities in excess of 95%. It is instructive to consider

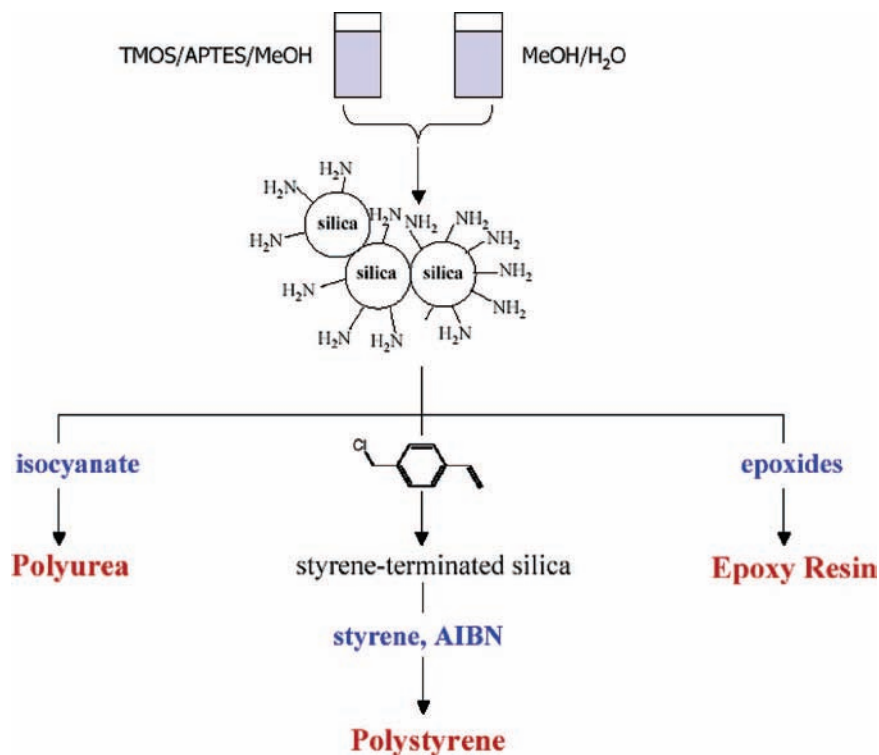


FIGURE 7. Selected cross-linking possibilities for amine-modified silica.

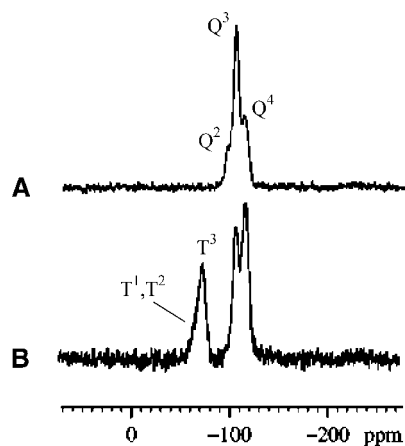


FIGURE 8. CP-MAS <sup>29</sup>Si NMR of aerogels made with TMOS (A) and a 3:1 TMOS:APTES volume ratio (B).

the DoE-predicted variation of strength with density for the same initial TMOS/APTES concentration at the two processing temperatures (Figure 10).<sup>28</sup> As dimensions do not change during processing, aerogels made with the same amount of silica and having the same final density contain the same amount of polymer, but aerogels cross-linked at 71 °C are consistently weaker (by up to 40%) than those made at room temperature (albeit making the latter takes longer). Therefore, the chemical makeup of the two polymers should be different. Given that native APTES-modified silica carries via TMOS Q<sup>3</sup> silicon atoms with hydroxyl groups (Figure 8B), and that TMOS-derived silica reacts with isocyanate reasonably fast only at elevated temperatures,<sup>16,17</sup> it is suggested that under standard

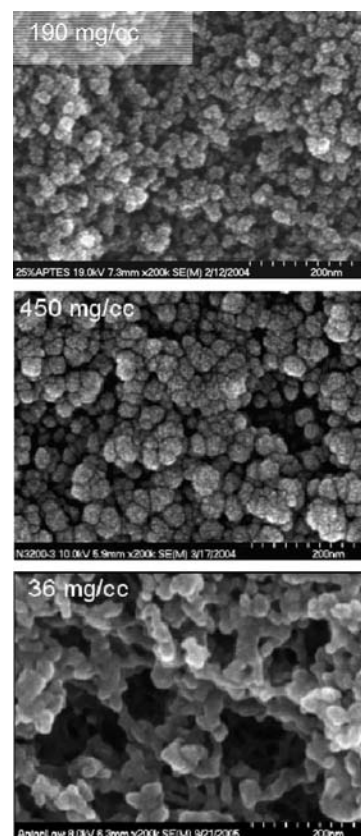
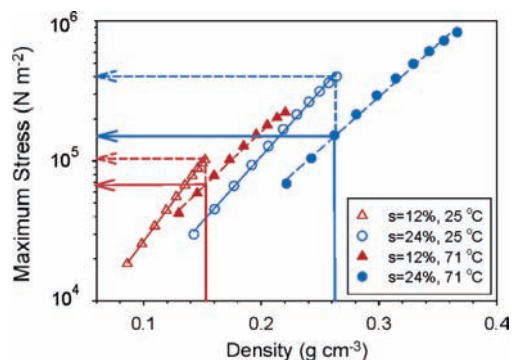


FIGURE 9. Comparative SEM of a standard (see the text) native TMOS/APTES aerogel (top), a higher-density cross-linked sample (middle), and a lower-density cross-linked sample (bottom). Middle and bottom panels reprinted from ref 28, Copyright 2006, with permission from Elsevier.



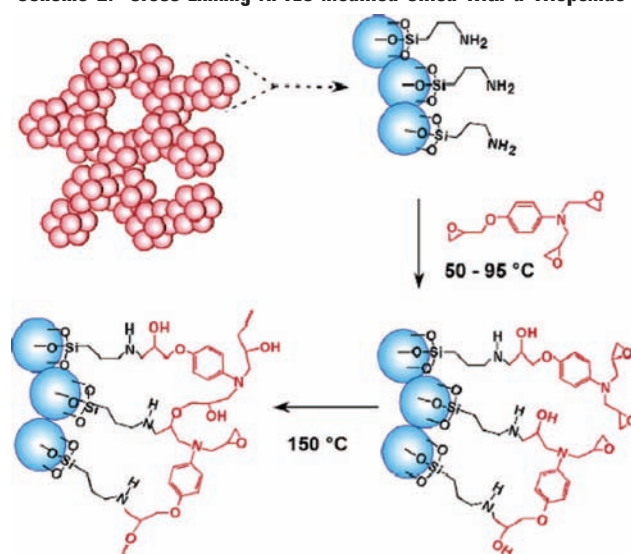
**FIGURE 10.** Predicted plots of maximum stress vs density using model-generated data points at 12% (red) and 24% (blue) of total silane (TMOS/APTES) (v/v) in  $\text{CH}_3\text{CN}$ . Empty symbols depict data for aerogels made at 25 °C; filled symbols depict data for aerogels made at 71 °C. Monoliths produced at 71 °C are predicted to be always weaker than monoliths of the same density (i.e., along the vertical lines) made at 25 °C. Reprinted from ref 28, Copyright 2006, with permission from Elsevier.

processing conditions ( $\sim 70$  °C) isocyanate most probably binds to APTES-modified silica via both carbamates and ureas.

Studies of the effect of the preparation conditions on the properties of cross-linked aerogels were partly motivated by the practical need to reduce the preparation time by reducing or eliminating the number of postgelation washes. In one school of thought, this may be accomplished by reaching a balance between the (TMOS/APTES):isocyanate and (TMOS/APTES): $\text{H}_2\text{O}$  ratios. CP-MAS  $^{13}\text{C}$  NMR of cross-linked aerogels has shown that as the number of postgelation washes is decreased from four to none, the length of the polymer may increase from three hexamethylene repeat units (four washes) to more than 600 repeat units (no washes).<sup>21</sup> The porosity (by SEM) may also decrease as the amount of material taken up increases,<sup>21</sup> supporting the role of the gelation water in the cross-linking process.

**3.a.2. Cross-Linking with Epoxies.** In analogy to isocyanate cross-linking that mimics polyurethane chemistry, we have also imitated “epoxy glue” chemistry where amine-modified silica plays the role of the hardener reacting with a multifunctional epoxide.<sup>30</sup> Epoxy-cross-linked aerogels based on the standard TMOS/APTES formulation may have a density of up to  $0.49\text{ g/cm}^3$  with a BET surface area of  $314\text{ m}^2/\text{g}$  and an average pore diameter of  $14.7\text{ nm}$ . CP-MAS  $^{13}\text{C}$  NMR excludes interparticle tethers from ring opening homopolymerization of epoxides, supporting the cross-linking mechanism of Scheme 2. Again DoE studies were used to investigate the role of parameters such as the “valency” of the epoxide in materials properties. Figure 11 summarizes data for density, ultimate strength, and modulus (by a three-point bend test) as a function of preparation conditions. Consistently, triepoxide-cross-linked aerogels exhibit higher density, strength, and stiffness for almost all preparation conditions. This may be related to either the reactivity of the epoxide or its structure. Interestingly, for all epoxides, density and modulus vary in a similar fashion, indicating that the elastic modulus increases monotonically with

**Scheme 2. Cross-Linking APTES-Modified Silica with a Triepoxide<sup>a</sup>**



<sup>a</sup> Reprinted with permission from ref 30. Copyright 2005 American Chemical Society.

density for any formulation. This is rather expected as interparticle necks become stiffer when material accumulates on the particles. On the other hand, however, the stress at failure shows a clear maximum, presumably corresponding to the maximum degree of interparticle cross-linking. Strength and modulus data taken together have been considered as strong evidence of the role of building interparticle tethers for strength. Similar trends with analogous inferences have been reported recently for aerogels cross-linked with isocyanate derived polymers.<sup>21b</sup>

**3.a.3. Cross-Linking with Polystyrene.** Although isocyanate and epoxy-cross-linked aerogel monoliths are much less hydrophilic than native silica, they are not hydrophobic: for instance, in contact with water, they are quickly filled with the liquid and sink within minutes. This is not surprising because both polyurethanes and epoxies have polar groups able to hydrogen bond with water. To impart hydrophobicity, nonpolar cross-linkers such as polystyrene and polypentafluorostyrene were considered.<sup>31</sup> The cross-linking process was rather lengthy (Scheme 3). First, amines of standard APTES-modified silica reacted with *p*-chloromethylstyrene; subsequently, styrene or pentafluorostyrene and a free radical initiator (AIBN) were introduced into the mesopores, and the samples were heated. The free radical process initiated in the mesopores engages surface-bound styrene, and when radicals at the tips of polymer chains growing out from the surface meet, the radical process is terminated, yielding molecular interparticle tethers. In fact, this process is not in principle different from the peroxide-initiated copolymerization of methacrylate with surface-bound methacrylate [introduced by cogelation of an epoxysilane, methacryloxysilane, and  $\text{T}(\text{OR})_4$ ], described in the mid-1980s by Schmidt for contact lens applications.<sup>34</sup> In our case, however, unbound polymer formed in the mesopores was removed by post-cross-linking washes, and wet gels were dried to aerogels.<sup>31</sup> Polystyrene-cross-linked aerogels are strong mechanically in analogy to their isocyanate and

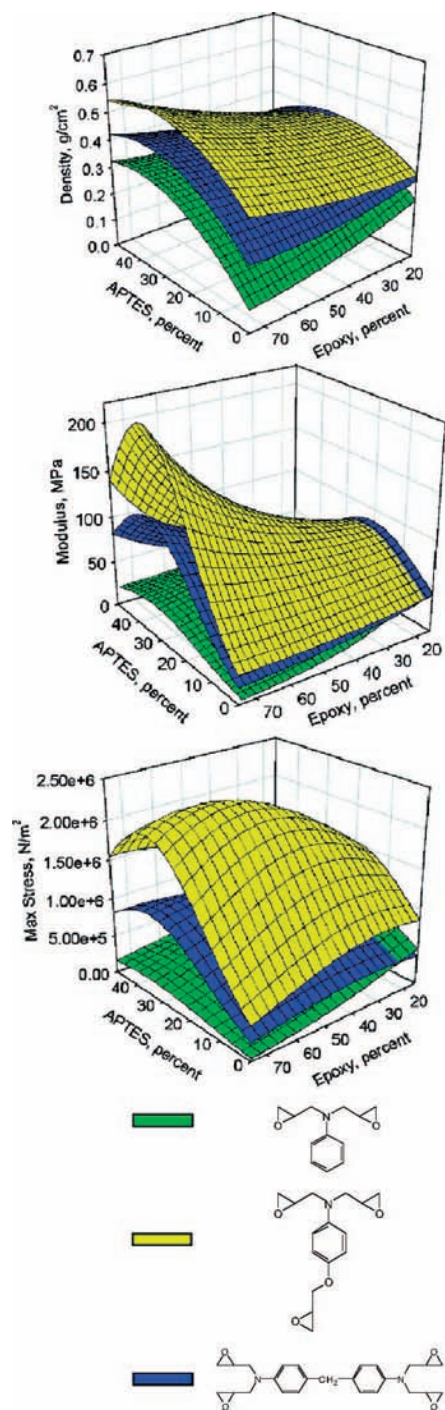
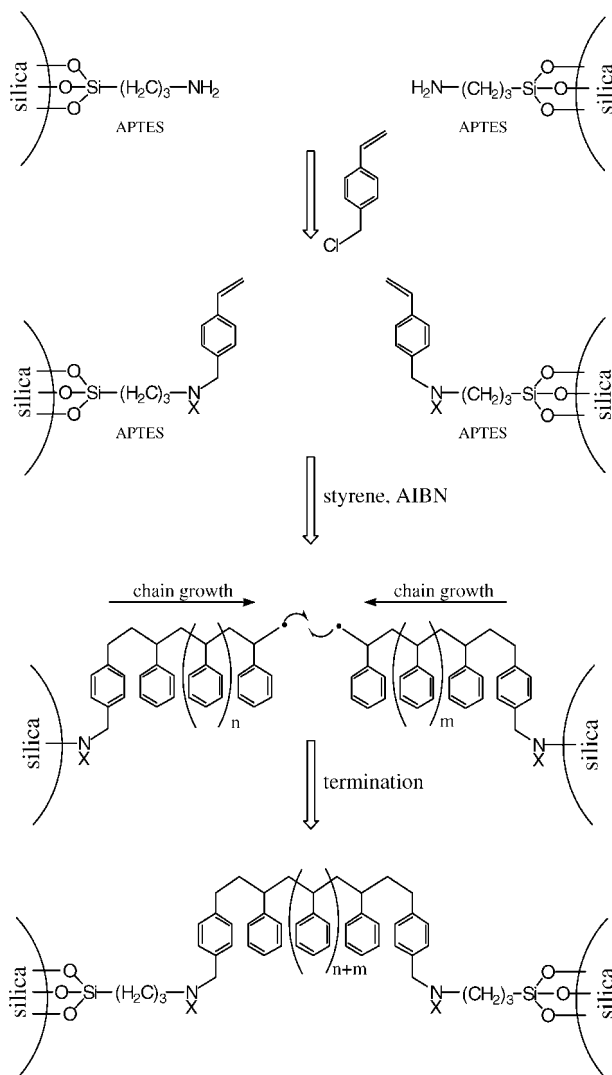


**FIGURE 11.** Response surface models for density, modulus, and stress at failure (via a short-beam bending test method) of epoxy-cross-linked silica aerogels vs APTES and epoxide concentration with cross-linking time and bath temperature held constant at the predicted optimum value for stress at failure.

epoxy counterparts. Typical monoliths with a bulk density of  $0.47 \text{ g/cm}^3$  show a relative high BET surface area ( $370 \text{ m}^2/\text{g}$ ), pore diameters of  $\sim 11.5 \text{ nm}$ , and a thermal conductivity of  $0.041 \text{ W m}^{-1} \text{ K}^{-1}$ . The average surface-bound polymeric tether consists of 15 monomer units (determined by both  $^{13}\text{C}$  NMR and density change considerations) with a polydispersity of 2.05 (determined by GPC), which is higher than that of the free polymer formed in the mesopores (1.50),

**Scheme 3.** Cross-Linking of APTES-Modified Silica Nanoparticles with Polystyrene<sup>31</sup>



reflecting a bimodal radical termination process in which surface-surface and surface-solution radical combination events form shorter and longer polymer chains, respectively.

Water droplets on isocyanate-cross-linked aerogel disks form a contact angle of  $59.7 \pm 1.3^\circ$  and are absorbed by the pores within 5 min. With polystyrene-cross-linked disks, the contact angle is  $121.4 \pm 0.9^\circ$ , and with polypentafluorostyrene, it is  $151.3 \pm 1.8^\circ$ . Those contact angles do not change with time, and polystyrene-cross-linked aerogel monoliths float on water for months.<sup>31</sup>

**3.b. Effect of the Network Morphology on Strength.** Acid-catalyzed silica aerogels have a polymer-like (fibrous), as opposed to the colloidal (particulate) texture of their base-catalyzed counterparts,<sup>6</sup> and they are twice as stiff.<sup>35</sup> Therefore, it was reasoned that by varying the chemical identity of the aerogel framework, we could potentially realize not only materials with variable optical, electrical, magnetic, and chemical (e.g., catalytic) properties without a need for external doping,<sup>36</sup> but also different elements that would yield network morphologies that could dissipate load forces differently, resulting in yet stronger materials. In that context, we were aware of the



wormlike texture of vanadia aerogels.<sup>37</sup> Thus, in addition to silica, we prepared and isocyanate-cross-linked aerogels based on 30 other elements from the periodic table (Al, Sc, Ti, V, Cr, Mn, Fe, Y, Zr, Nb, Ru, In, La, Pr, Nd, Sm, Eu, Gd, Tb, Dy, Ho, Er, Tm, Yb, Lu, Hf, Ta, W, and Re). As it turns out, even gels prepared from hydrated metal chlorides via a nonhydrolytic route<sup>38</sup> are surface-terminated with OH groups and retain coordination water so that they are able to develop conformal polymer coatings by reaction with di- and triisocyanates in analogy with silica. Rare earth (RE) aerogels were studied in greater detail because of their dielectric and paramagnetic properties.<sup>40</sup> They are nonstoichiometric amorphous materials with moderately high surface areas ( $368 \pm 14 \text{ m}^2/\text{g}$  before and  $156 \pm 19 \text{ m}^2/\text{g}$  after cross-linking). The percent metal content ( $58.0 \pm 2.3\%$ , w/w) is significantly lower than that of pure oxides ( $85.4\text{--}87.9\%$ , w/w). Even native RE aerogels contain a significant amount of carbon, mostly as carbonate ( $9.0 \pm 2.4\%$ , w/w), presumably formed during SCF drying. The gram magnetic susceptibility,  $\chi$ , is a sensitive probe of the skeletal contribution to the materials properties. Aerogels have  $\chi$  values lower than those of the corresponding xerogels, because of the higher carbonate content. Cross-linked aerogels exhibit  $\chi$  values lower than those of both xerogels and aerogels, reflecting spin dilution by the polymer (Figure 12A). Despite their stoichiometric complexity, the magnetic susceptibility of RE aerogels varies linearly with the susceptibility of the pure oxides (Figure 12B), as if RE aerogels were pure compounds themselves, a property potentially very useful from an applications design perspective.

Microscopically, with the exception of vanadia, all non-silica aerogels look very similar to one another, consisting of nanoparticles, pretty much like the base-catalyzed silica of Figure 1, and the mechanical properties track those of cross-linked silica. Vanadium aerogels consist of entangled wormlike nanosized objects assembled into a bird nest-like structure (Figure 13A).<sup>37</sup> Cross-linking vanadia aerogels with isocyanate yields a conformal coating (Figure 13B).

Cross-linked vanadia aerogels possess very interesting mechanical properties (Figure 14).<sup>41</sup> Isocyanate-cross-linked APTES-modified silica aerogels ( $0.48 \text{ g}/\text{cm}^3$ ) fail at 77% strain under  $\sim 30$  ksi compression, but vanadia ( $0.38 \text{ g}/\text{cm}^3$ ) does not fail even at 95% compressive strain under 100 ksi. Samples do not buckle, and swell only at the very last stages of compression (Poisson ratio = 0.18). The material is practically absorbed by its own porosity. Samples recovered after testing show a complete loss of their internal surface area. From an applications perspective, a very important property of those materials is their ability to store energy, particularly at high strain rates. Thus, the specific energy absorption density of isocyanate-cross-linked vanadia ( $0.52 \text{ g}/\text{cm}^3$ ) is  $1.3 \times 10^6 \text{ N m kg}^{-1}$ . By comparison, the energy absorption density at the fail point of isocyanate-cross-linked silica ( $0.48 \text{ g}/\text{cm}^3$ ) is  $7.3 \times 10^4 \text{ N m kg}^{-1}$ , and that of armor grade SiC-N

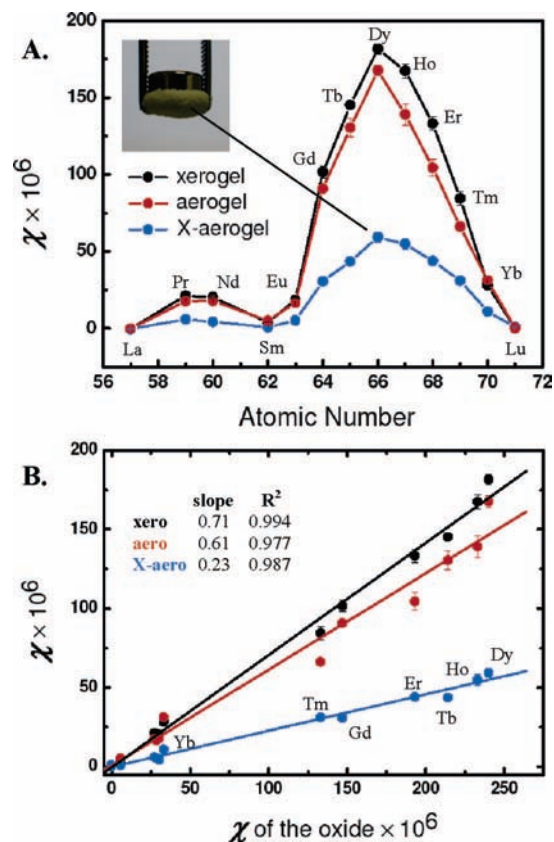


**FIGURE 12.** Room-temperature gram magnetic susceptibilities,  $\chi$ , of rare earth sol-gel materials as a function of the atomic number showing the expected trend for pure compounds (A). Those  $\chi$ -values in fact correlate linearly with the susceptibilities of the pure oxides (B), reflecting the stoichiometric similarity within each series of materials. Slopes are proportional to the relative abundance of the metal ions. The inset in panel A shows the X-dysprosium aerogel powder picked up by a 1 cm diameter Nd-Fe-B magnet. Reprinted with permission from ref 40. Copyright 2007 The Royal Society of Chemistry.

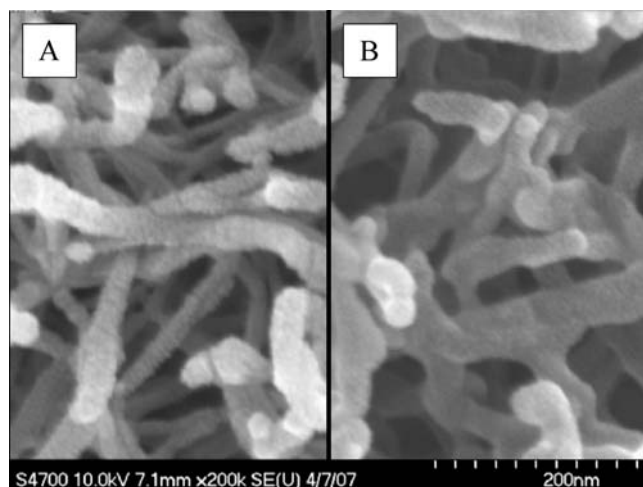


**FIGURE 13.** SEM of (A) a native vanadia aerogel ( $\rho_b = 0.078 \text{ g}/\text{cm}^3$ ) and (B) a vanadia aerogel cross-linked with diisocyanate ( $\rho_b = 0.428 \text{ g}/\text{cm}^3$ ).

ceramics is  $3.5 \times 10^4 \text{ N m kg}^{-1}$ , namely  $\sim 50$  times lower than that of the  $0.52 \text{ g}/\text{cm}^3$  cross-linked vanadia aerogels.<sup>39</sup>

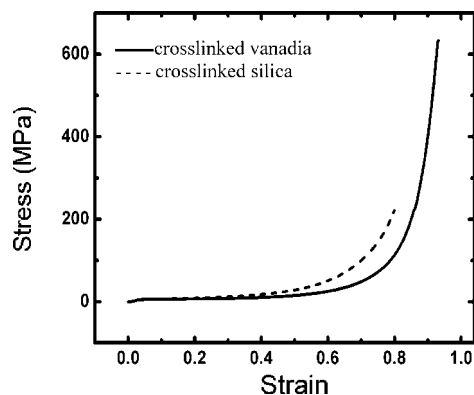


**FIGURE 14.** Comparative quasi-static compression data for silica ( $\rho_b = 0.48 \text{ g/cm}^3$ ) and vanadia-cross-linked aerogels ( $\rho_b = 0.38 \text{ g/cm}^3$ ).

#### 4. Summary and Outlook

Templated nanocasting of polymeric cross-linkers on the skeletal superstructure of typical aerogels is emerging as an efficient method for imparting strength with minimum compromise in the internal porosity. Polymer-cross-linked aerogels are clearly multifunctional materials that combine at the very least high mechanical strength with low thermal conductivity. In terms of strength, there is a clear correlation with the nanostructure morphology (case of silica versus vanadia), which must be understood via theory and simulation for more efficient materials design. Nevertheless, even from a purely phenomenological perspective, it appears that cross-linked aerogels already compete favorably with other strong materials. The question then is whether the technology is ready for production. Currently, the major practical concern is the length of the preparation process that still involves several time-consuming solvent exchange steps. That may limit use to high-value-added applications, for example, in monolithic separation media (HPLC columns and filtration membranes) or perhaps even guided drug delivery (the case of magnetic rare earth aerogels). Large-volume applications, such as architectural thermal and acoustic insulation, would require a shorter preparation process. In our view, streamlined processing is intimately related to chemistry, and the major issue then is to deconvolute the cross-linking from the gelation chemistry so that all reagents will be mixed together from the beginning. Furthermore, our preferred approach to free ourselves from having to develop a new surface chemistry for every new polymer under consideration is, instead of decorating the inorganic framework with monomers, to create a generic surface that under carefully controlled conditions will bind all available monomer, eliminating the need for time-consuming post-cross-linking washes. Overall, there is plenty of room for creative thinking and a lot of practical potential for this new class of materials.

Support from the NASA GRC Science Advisory Board and the University of Missouri Research Board is gratefully acknowledged. I also thank my many collaborators at the University of Missouri, NASA GRC, and Oklahoma State University who have made cross-linked aerogels (X-aerogels) possible: Antonella Alunni, Lynn

Capadona, Joe Counsel, Paul Curto, Amala Dass, Eve Fabrizio, Abigail Hobbs, U. Faysal Ilhan, J. Chris Johnston, Jim Kinder, Hongbing Lu, Linda McCorkle, Mary Ann Meador, Sudhir Mulik, Anna Palczer, Abdel-Monem Rawashdeh, Samit Roy, Dan Scheiman, Jennifer Schnobrich, Chariklia Sotiriou-Leventis, Jeff Thomas, Plousia Vassilaras, Xiaojiang Wang, and Guohui Zhang.

#### References

- (1) Thayer, A. M. Nanomaterials. *Chem. Eng. News* **2003**, *81*, 15–22.
- (2) Ahmad, Z.; Mark, J. E. Polyimide-ceramic hybrid composites by the sol-gel route. *Chem. Mater.* **2001**, *13*, 3320–3330.
- (3) Mitchell, C. A.; Bahr, J. L.; Arepalli, S.; Tour, J. M.; Krishnamoorti, R. Dispersion of functionalized carbon nanotubes in polystyrene. *Macromolecules* **2002**, *35*, 8825–8830.
- (4) Rolison, D. Catalytic nanoarchitectures: The importance of nothing and the unimportance of periodicity. *Science* **2003**, *299*, 1698–1701.
- (5) According to IUPAC, mesopores fall in the range of 2–50 nm: Sing, K. S. W.; Everett, D. H.; Haul, R. A. W.; Moscou, L.; Pierotti, R. A.; Rouquerol, J.; Siemieniewska, T. Reporting physisorption data for gas/solid systems with special reference to the determination of surface area and porosity (recommendations 1984). *Pure Appl. Chem.* **1985**, *57*, 603–619.
- (6) Brinker, C. J.; Scherer, G. W. *Sol-gel science. The physics and chemistry of sol-gel processing*; Academic Press: New York, 1990.
- (7) Husing, N.; Schubert, U. Aerogels-airy materials: Chemistry, structure, and properties. *Angew. Chem., Int. Ed.* **1998**, *37*, 22–45.
- (8) Pierre, A. C.; Pajonk, G. M. Chemistry of aerogels and their applications. *Chem. Rev.* **2002**, *102*, 4243–4265.
- (9) There are notable exceptions where SCF drying has been replaced by freeze-drying or ambient-pressure drying of hydrophobic aerogels via the so-called spring back effect. See for example: Prakash, S. S.; Brinker, C. J.; Hurd, A. J.; Rao, S. M. Silica aerogel films prepared at ambient pressure by using surface derivatization to induce reversible drying shrinkage. *Nature* **1995**, *374*, 439–443.
- (10) Hrubesh, L. W.; Poco, J. F. Thin aerogel films for optical, thermal, acoustic and electronic applications. *J. Non-Cryst. Solids* **1995**, *188*, 46–53.
- (11) Gross, J.; Fricke, J. Ultrasonic velocity measurements in silica, carbon and organic aerogels. *J. Non-Cryst. Solids* **1992**, *145*, 217–222.
- (12) Gibson, L. J.; Ashby, M. F. *Cellular solids: Structure and properties*, 2nd ed.; Cambridge University Press: Cambridge, U.K., 1997.
- (13) Hæreid, S.; Anderson, J.; Einarsrud, M. A.; Hua, D. W.; Smith, D. M. Thermal and temporal aging of TMOS-based aerogel precursors in water. *J. Non-Cryst. Solids* **1995**, *185*, 221–226.
- (14) Lucas, E. M.; Doescher, M. S.; Ebenstein, D. M.; Wald, K. J.; Rolison, D. R. Silica aerogels with enhanced durability, 30-nm mean pore-size, and improved immersibility in liquids. *J. Non-Cryst. Solids* **2004**, *350*, 244–252.
- (15) Leventis, N.; Sotiriou-Leventis, C. Methods and compositions for preparing silica aerogels U.S. Patent Application 20040132846 2004.
- (16) Leventis, N.; Sotiriou-Leventis, C.; Zhang, G.; Rawashdeh, A.-M. M. Nanoengineering strong silica aerogels. *Nano Lett.* **2002**, *2*, 957–960.
- (17) Zhang, G.; Dass, A.; Rawashdeh, A.-M. M.; Thomas, J.; Counsel, J. A.; Sotiriou-Leventis, C.; Fabrizio, E. F.; Ilhan, F.; Vassilaras, P.; Scheiman, D. A.; McCorkle, L.; Palczer, A.; Johnston, J. C.; Meador, M. A. B.; Leventis, N. Isocyanate-crosslinked silica aerogel monoliths: Preparation and characterization. *J. Non-Cryst. Solids* **2004**, *350*, 152–164.
- (18) Lowen, W. K.; Broge, E. C. Effects of dehydration and chemisorbed materials on the surface properties of amorphous silica. *J. Phys. Chem.* **1961**, *65*, 16–19.
- (19) Leventis, N.; Palczer, A.; McCorkle, L.; Zhang, G.; Sotiriou-Leventis, C. Nanoengineered silica-polymer composite aerogels with no need for supercritical fluid drying. *J. Sol-Gel Sci. Technol.* **2005**, *35*, 99–105.
- (20) Brinker, C. J.; Keefer, K.; Schaefer, D. W.; Assink, R. A.; Kay, B. D.; Ashley, C. S. Sol-gel transition in simple silicates. II. *J. Non-Cryst. Solids* **1984**, *63*, 45–59.
- (21) (a) Meador, M. A. B.; Capadona, L. A.; Vassilaras, P.; Leventis, N. Effect of processing conditions on chemical make-up of diisocyanate crosslinked silica aerogels. *Polym. Prepr. (Am. Chem. Soc., Div. Polym. Chem.)* **2006**, *47*, 384–385. (b) Meador, M. A. B.; Capadona, L. A.; McCorkle, L.; Papadopoulos, D. S.; Leventis, N. Structure-property relationships in porous 3D nanostructures as a function of preparation conditions: Isocyanate cross-linked silica aerogels. *Chem. Mater.* **2007**, *19*, 2247–2260.

- (22) Ellsworth, M. W.; Novak, B. M. Mutually interpenetrating inorganic-organic networks. New routes into nonshrinking sol-gel composite materials. *J. Am. Chem. Soc.* **1991**, *113*, 2756–2758.
- (23) Novak, B. M.; Auerbach, D.; Verrier, C. Low-density, mutually interpenetrating organic-inorganic composite materials via supercritical drying techniques. *Chem. Mater.* **1994**, *6*, 282–286.
- (24) Einarsrud, M. A.; Kirkedelen, M. B.; Nilsen, E.; Mortensen, K.; Samseth, J. Structural development of silica gels aged in TEOS. *J. Non-Cryst. Solids* **1998**, *231*, 10–16.
- (25) Kramer, S. J.; Rubio-Alonso, F.; Mackenzie, J. D. Organically modified silicate aerogels, “aeromossils”. *Mater. Res. Soc. Symp. Proc.* **1996**, *435*, 295–300.
- (26) Hu, Y.; Mackenzie, J. D. Rubber-like elasticity of organically modified silicates. *J. Mater. Sci.* **1992**, *27*, 4415–4420.
- (27) Katti, A.; Shimpi, N.; Roy, S.; Lu, H.; Fabrizio, E. F.; Dass, A.; Capadona, L. A.; Leventis, N. Chemical, physical and mechanical characterization of isocyanate-crosslinked amine-modified silica aerogels. *Chem. Mater.* **2006**, *18*, 285–296.
- (28) Capadona, L. A.; Meador, M. A. B.; Aluni, A.; Fabrizio, E. F.; Vassilaras, P.; Leventis, N. Flexible, low-density polymer crosslinked silica aerogels. *Polymer* **2006**, *47*, 5754–5761.
- (29) Luo, L.; Lu, H.; Leventis, N. The compressive behavior of isocyanate crosslinked silica aerogels at high strain rates. *Mech. Time-Depend. Mater.* **2006**, *10*, 83–111.
- (30) Meador, M. A. B.; Fabrizio, E. F.; Ilhan, F.; Dass, A.; Zhang, G.; Vassilaras, P.; Johnston, J. C.; Leventis, N. Crosslinking amine-modified silica aerogels with epoxies: Mechanically strong lightweight porous materials. *Chem. Mater.* **2005**, *17*, 1085–1098.
- (31) Ilhan, F. U.; Fabrizio, E. F.; McCorkle, L.; Scheiman, D. A.; Dass, A.; Palczer, A.; Meador, M. A. B.; Johnston, J. C.; Leventis, N. Hydrophobic monolithic aerogels by nanocasting polystyrene on amine-modified silica. *J. Mater. Chem.* **2006**, *16*, 3046–3054.
- (32) Hüsing, N.; Schubert, U.; Mezei, R.; Fratzl, P.; Riegel, B.; Kiefer, W.; Kohler, D.; Mader, W. Formation and structure of gel networks from  $\text{Si}(\text{OEt})_4/(\text{MeO})_3\text{Si}(\text{CH}_2)_3\text{NR}_2'$  mixtures ( $\text{NR}_2' = \text{NH}_2$  or  $\text{NHCH}_2\text{-CH}_2\text{NH}_2$ ). *Chem. Mater.* **1999**, *11*, 451–457.
- (33) Shigley, J. E.; Mischke, C. R. M. *Mechanical Engineering Design*, 6th ed.; : New York, 2001; p 1206.
- (34) Philipp, G.; Schmidt, H. New materials for contact lenses prepared from Si- and Ti-alkoxides by the sol-gel process. *J. Non-Cryst. Solids* **1984**, *63*, 283–292.
- (35) Woignier, T.; Phalippou, J.; Vacher, R. Parameters affecting elastic properties of silica aerogels. *J. Mater. Res.* **1989**, *4*, 688–692.
- (36) Morris, C. A.; Anderson, M. L.; Stroud, R. M.; Merzbacher, C. I.; Rolison, D. R. Silica sol as a nanoglue: Flexible synthesis of composite aerogels. *Science* **1999**, *284*, 622–624.
- (37) Sudant, G.; Baudrin, E.; Dunn, B.; Tarascon, J.-M. Synthesis and electrochemical properties of vanadium oxide aerogels prepared by a freeze-drying process. *J. Electrochem. Soc.* **2004**, *151*, A666–A671.
- (38) Gash, A. E.; Tillotson, T. M.; Satcher, J. H., Jr.; Hrubesh, L. W.; Simpson, R. L. New sol-gel synthetic route to transition and main-group metal oxide aerogels using inorganic salt precursors. *J. Non-Cryst. Solids* **2001**, *285*, 22–28.
- (39) Luo, H.; Chen, W.; Rajendran, A. M. Dynamic compressive response of damaged and interlocked SiC-N ceramics. *J. Am. Ceram. Soc.* **2006**, *89*, 266–273.
- (40) Leventis, N.; Vassilaras, P.; Fabrizio, E. F.; Dass, A. Polymer nanoencapsulated rare earth aerogels: Chemically complex but stoichiometrically similar core-shell superstructures with skeletal properties of pure compounds. *J. Mater. Chem.* **2007**, *17*, 1502–1508.
- (41) Luo, H.; Gitogo, G.; Lu, H.; Schnobrich, J.; Hobbs, A.; Fabrizio, E. F.; Dass, A.; Mulik, S.; Leventis, N. Physical, chemical and mechanical characterization of isocyanate cross-linked vanadia aerogels. Submitted.

AR600033S